Hyperspectral Ait-to-Air Seeker

Nahum Gat

Opto-Knowledge Systems, Inc. (OKSI)
1227 Ninth Street, Manhattan Beach, CA 90266-6017
Telephone: 310/376-6078 *Fax*: 310/379-9842 *e-mail*: oksi @ nic.cerf.net

Jacob Barhen, and Sandeep Gulati

Jet Propulsion Laboratory, California Institute of Technology, Pasadena, CA

Capt. Todd D. Steiner

U.S. Air Force, Wright Laboratory (WL/MNGS), Eglin AFB, FL

ABSTRACT

Synthetic hyperspectral signatures representing an airborne target engine radiation, a decoy flare, and the engine plume radiation are used to demonstrate computational techniques for the discrimination between such objects. Excellent discrimination is achieved for a "single look" at SNR of -10dB. Since the atmospheric transmittance perturbs the signature of all objects in an identical fashion, the transmittance is equivalent to a modulation of the target radiance (in the spectral domain). The proper spectral signal decomposition may, therefore, recover the original unperturbed signature accurately enough to allow discrimination. The algorithms described here, and in two accompanying papers, have been tested over the spectral range that includes the VNIR and MWIR and are most appropriate for an intelligent, autonomous, air-to-air or surface-to-air guided munitions. With additional enhancements, the techniques apply to ground targets and other dual-use applications.

1 INTRODUCTION

The subject addressed in this paper is related to the utilization of hyperspectral signatures for the classification of objects, with specific emphasis on the discrimination of targets from countermeasures in airborne applications. In this investigation, **hyperspectral techniques** refer to two topics, which are defined as follows.

1. A signature that is expressed as a function of wavelength, often in a large number of contiguous bands, is referred to as hyperspectral signature, obtained via a hyperspectral sensor. This aspect of the definition is in contrast to multispectral techniques in which the signature is expressed in a (small) number of discrete bands.

2. The second aspect of the definition is related to mathematical operations in which the signature in the spectral domain is operated upon by various mathematical transforms. The signature is said, in this case, to be transformed into a hyperspectral domain, allowing treatment akin to the familiar time-spectrum domain analyses (e.g., Fourier Transform). Based on context, there is little chance for confusion as to which aspect of the definition is used.

Pseudo spectrum, or **pseudo signature** of a target, is defined as a contiguous spectrum, constructed from the original signature by selecting discrete spectral (not necessarily contiguous) bands (not necessarily of uneven bandwidth). The collection of such discrete and non uniform bands into a pseudo spectrum allows the application of all common signal processing mathematical tools for the purpose of

0-8194-1535-9/94/$6.00

signature analysis. The optimal selection of which, and how many, bands to be included in the pseudo signature of a target is another object of the present investigation. The robustness of the target/decoy discrimination is found to directly depend on the proper and judicious selection of these bands, and some important trade-offs must be addressed. To emphasize, in the present investigation we limited ourselves to target/decoy discrimination, assuming that the seeker has already locked onto the target; we do not deal with search and target acquisition. Furthermore, we are not dealing with the probabilistic framework of decision making and hypothesis testing. Thus, we do not consider probability of detection nor false alarm rates.

Several approaches were considered for target/decoy discrimination, all are performed in the hyperspectral domain. The approaches discussed here are based on autocorrelation, matched filter discriminator, and singular value decomposition (SVD) techniques. We recognize that such technique may be computationally expensive. A discrimination algorithm that also results in a robust discrimination and is much faster, is based on a similar technique, orthogonal subspace projection, and is described in a concurrent set of papers.[1,2] Reference 2 also discusses an approach for rapid atmospheric deconvolution for the pseudo spectrum of targets.

In the following analysis, we use synthetic signatures generated via the application of LOWTRAN or MODTRAN in conjunction with a radiation source. For simplicity, the target (or engine) is assumed a Planckian radiator at about 800 K, the plume radiance is calculated via LOWTRAN by specifying a layer of hot gas (with H_2O and CO_2 contents corresponding to the stoichiometric combustion of jet fuel) at about 600 K, and a decoy flare is assumed a Planckian radiator at 2,000K.

2 ANALYSIS

We begin with some preliminary definitions and assumptions to characterize the computational framework. We conclude by addressing extensions that might be required to increase the robustness of the methodology when handling data from actual sensors.

We assume that the sensor provides intensity readings in N spectral bands. For the purpose of discrimination, we require baseline (truth data) spectra for plume, engine, and flare corresponding to various engagement scenarios. In the sequel, we limit ourselves to a single configuration, and denote the quantities of interest as p_n, e_n and f_n (n = 0,..,N-1), respectively. Furthermore, let $\bar{\eta}$ represent a vector combining the noise and clutter inherent to the sensing paradigm.

The hyperspectral signature can then be written a

$$s_n = x_n + \eta_n \qquad \forall n \in [0, \quad N-1] \tag{1}$$

The unknown spectral components x_n may originate from any of the following observations:

$x_n = 0$	:	noise/clutter
$x_n = f_n$	:	flare
$x_n = e_n$	:	engine
$x_n = p_n$	:	plume
$x_n = p_n + e_n$	:	engine and plume

Our first order of business is to discriminate between a target [$x_n = e_n \, |p_n| \, e_n + p_n$] and a decoy [$x_n = f_n$].

2.1 Target-Decoy (Flare) Discrimination

The most critical step in any discrimination problem is the appropriate choice of a decision space. If each spectral pattern class corresponds to an "attractor" (using the language of nonlinear dynamical systems theory), one would like to choose, if possible, a space where the distances between attractors are maximized.

In the particular instance under consideration, the sensor provides data in the spectral domain. Discrimination could be attempted on such data directly. On the other hand, it is important to remember that noise and clutter are present, and, sometimes contribute at such strengths as to completely drawn the signatures. Therefore, a compelling incentive exists to carry out the discrimination in some transformed domain, where the impact of noise and clutter would be reduced.

Let Ω denote a spectral operator, chosen from a broad selection of well known transforms (i.e., Fourier, Hadamard, Hermite, Hilbert, ...). If Ω operates on spectral data, we say that it maps the spectral domain into a hyperspectral domain.

Without loss of generality, we can choose the following computational scheme

$$\Omega = \mathcal{A} \odot \mathcal{F} \tag{2}$$

Here $\mathcal{F}$ denotes a DFT (or a FFT), and $\mathcal{A}$ performs an auto correlation on the resulting complex hyperspectrum. Our approach, and typical results obtained, are illustrated in Figs. 1 and 2 that correspond to SNR of +10dB and -10dB per spectrometer data frame (i.e., "single look"), respectively.

The lower left quadrant displays the baseline synthetic spectra of the engine, the plume, and the flare. Contributions of noise and clutter in each spectral band are also plotted, on a common scale. The upper left quadrant shows the corresponding hyperspectra. The reader should note that these left-hand-side (LHS) quadrants are used for illustrative purposes only. Discrimination is carried out based upon the information displayed in the right-hand-side (RHS) quadrants. The lower RHS quadrant involves plots of the signals. In all these calculations the SNR refers to the signal-to-noise ratio where the noise power is referred to the combined engine and plume (but not flare) power.

$$s_n^a = f_n + \eta_n^a \tag{3}$$

and

$$s_n^b = y_n + \eta_n^b \tag{4}$$

where $y_n = \{o\,|e_n|\,p_n|\,e_n + p_n\}$. The random processes $\overline{\eta}^a$ and $\overline{\eta}^b$ are allowed to exhibit a variable degree of incoherence, to capture the fact that the difference in spatial location between target and decoy often results in different background contributions. The sensor actually measures either $\overline{s}^a$ or $\overline{s}^b$. The two quantities are plotted concomitantly in the lower RHS quadrant, to illustrate the difficulty of making a correct decision in the spectral domain when noise and clutter dominate.

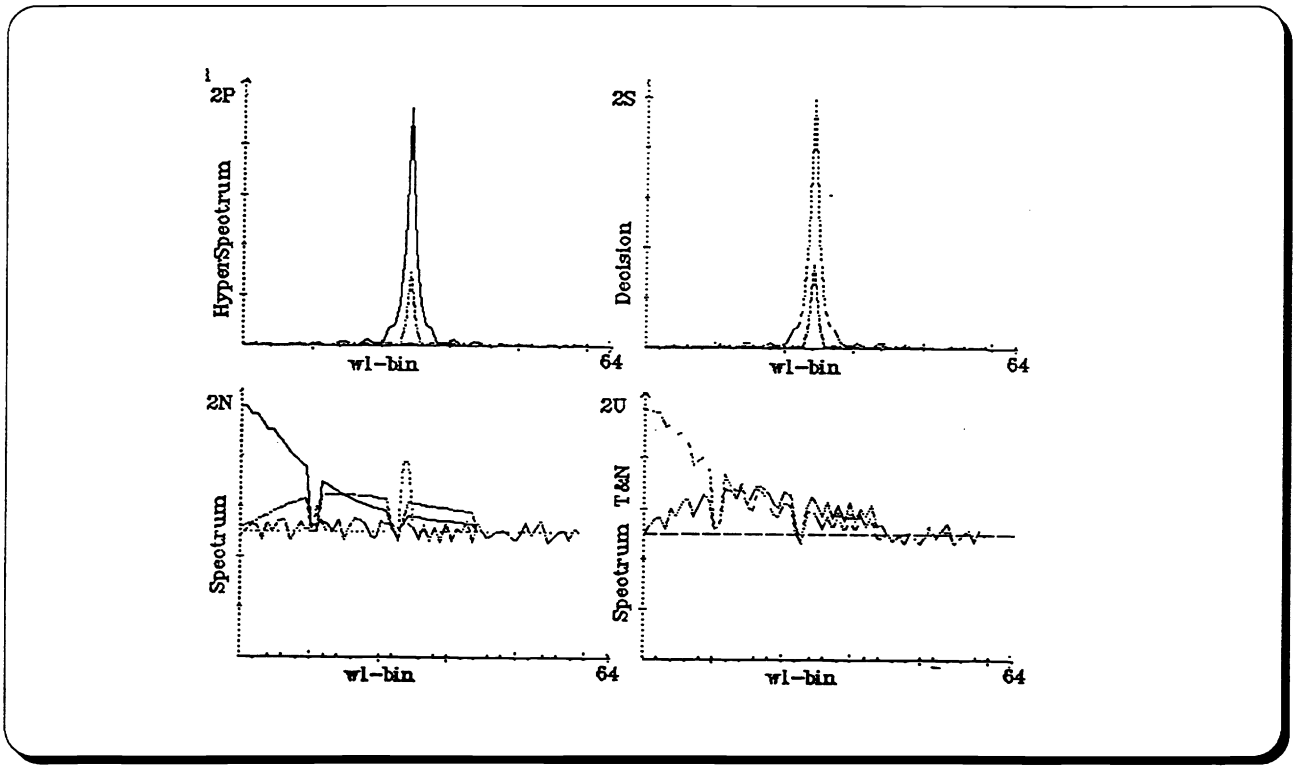

Figure 1. Target - Decoy Discrimination at S/N = 10 dB (Signal Source is the Engine).

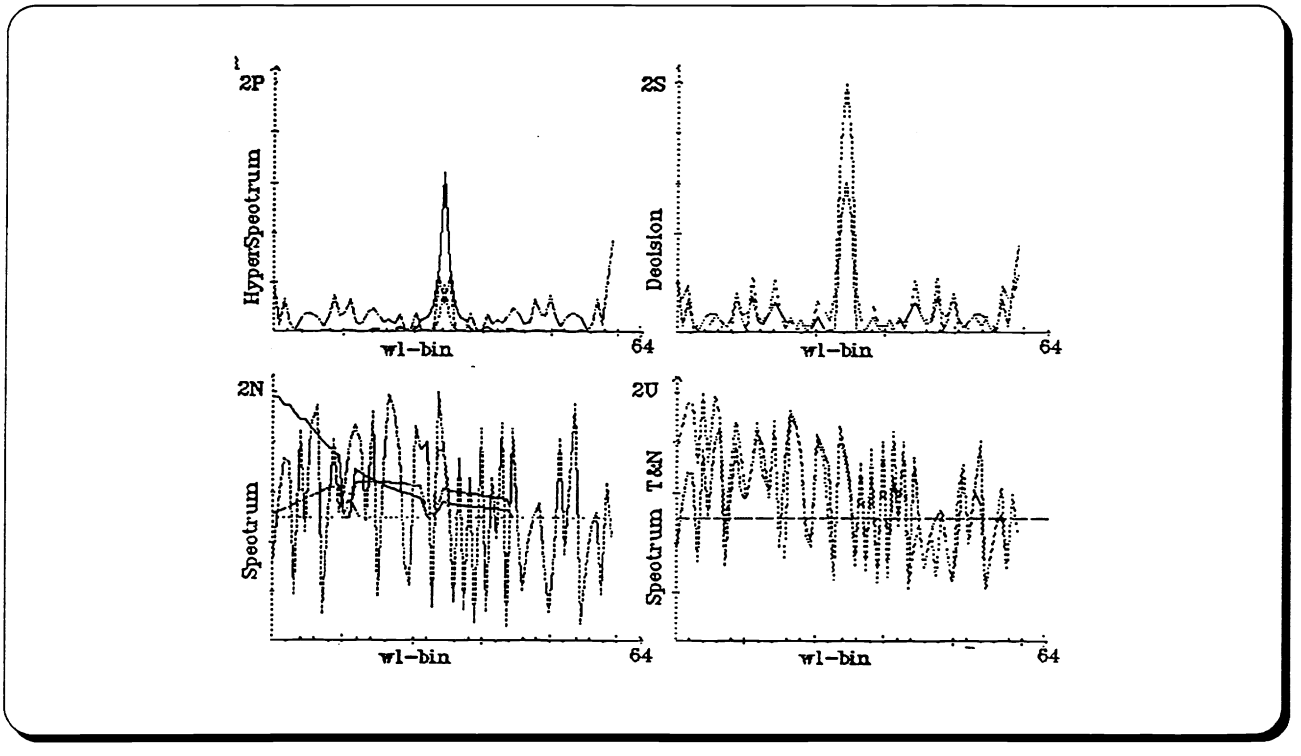

Figure 2. Target - Decoy Discrimination at S/N = -10 dB (Signal Source is the Engine).

The upper RHS quadrant presents the situation in the "decision" space. We have plotted the quantities

$$\bar{\sigma}^a = \Omega(\bar{s}^a) \tag{5}$$

and

$$\bar{\sigma}^b = \Omega(\bar{s}^b) \tag{6}$$

We observe that, even when the SNR drops to -10dB per frame, discrimination is easily performed. An important benefit resulting from the particular choice of Ω [viz Eq. (2)] is that dedicated microelectronics hardware implementation is straightforward.[3]

2.2 Plume-Engine Discrimination

At this stage we assume that the target-decoy discrimination has been successfully completed, and we focus on the surprisingly harder problem of distinguishing between engine and plume. Thus, our objective now is to determine, given the hyperspectral signature

$$s_n = y_n + \eta_n \tag{7}$$

the precise nature of the spectral source, i.e.,

$y_n = 0$	:	noise/clutter (miss target)
$y_n = e_n$	:	engine
$y_n = p_n$	:	plume
$y_n = p_n + e_n$	:	engine and plume

A number of different approaches could be explored in that context. First, we observe that the Ω operator [viz Eq. (2)], which can be successfully utilized to discriminate target from decoy, appears less sensitive to the spectral differences between engine and plume in the presence of strong noise and clutter interference [i.e., at SNRs < 5dB per frame]. We can construct a matched filter discriminator, building upon the classical computational scheme

$$C \odot [\mathcal{F}^{-1}\ (\hat{e}^* \cdot \hat{s}), \bar{e}] \tag{8}$$

$$C \odot [\mathcal{F}^{-1}\ (\hat{p}^* \cdot \hat{s}), \hat{p}] \tag{9}$$

etc... In the above expressions, the symbol $\odot$ denotes operator composition, C refers to correlation and $\mathcal{F}^{-1}$ stands for the inverse Fourier transform. Note that $\bar{e}^*$ and $\hat{p}^*$ are here the complex conjugates of the frequency inverted hyperspectra for the engine and plume, respectively. Computational experiments indicate that the discrimination power may be inadequate for SNRs under 10dB per frame.

The methodology that shows most promise, is based upon a powerful mathematical technique called "Singular Value Decomposition.[4]" In the most general case, given a complex-valued M x N matrix A of rank K, the SVD theorem states that there exist positive real numbers $\sigma_1 \geq \sigma_2 \geq \ldots \geq \sigma_k$ (the so-called singular values of A), an M x M unitary matrix U, and an N x N unitary matrix V, such that the matrix A can be expressed as

$$A = U \Sigma V^{\mathrm{H}} \tag{10}$$

where the M x N matrix has the structure

$$\Sigma = \begin{pmatrix} D & 0 \\ 0 & 0 \end{pmatrix} \tag{11}$$

and D = diag $[\sigma_1 \ldots \sigma_k]$ is a K x K diagonal matrix. In Eq. (10) V^H denotes the Hermitian of V. Using the SVD paradigm, we can construct the following discriminator. Consider the engine spectrum $\bar{e}$. We can define the engine spectral covariance matrix C_e as

$$C_e = \bar{e} \cdot \bar{e}^T \tag{12}$$

where the superscript T denotes transposition. More robustly, if noise and clutter estimates in the appropriate field of view can be readily obtained, we will set

$$C_e = E \cdot E^T \tag{13}$$

where

$$E = (\bar{e}^{(1)}, \ldots, \bar{e}^{(k)}) \tag{14}$$

and

$$\bar{e}^{(k)} = \bar{e} + \bar{\eta}^{(k)} \tag{15}$$

In the above expressions, k (k = 1,...,K) indexes spatial resolution cells from which noise/clutter estimates are measured.

In a similar vein we can construct covariance matrices for $\bar{p}$, $(\bar{p} + \bar{e})$, and $\bar{s}$. We will then carry out singular value decomposition of C_e, C_p, C_{p+e} and C_s to obtain the vectors $\bar{\sigma}^z$ $(z = e, p, \eta, s)$. The discrimination decision will be based upon an appropriate comparison of the $\bar{\sigma}^z$ vectors (e.g., matched filter, correlation). This approach should show quite successful at low SNRs (down to approximately -10dB per frame) as is illustrated in Fig. 3. The reader should note the differences in the information displayed from the previous figures. The lower LHS quadrant is unchanged. The upper LHS quadrant now displays the $\bar{\sigma}^z$ vectors $(z = e, p, \eta, s)$. The lower RHS quadrant portrays the signal measured by the sensor, while the upper RHS quadrant plots the baseline spectrum corresponding to the detection decision reached. It should be noted that the terminal guidance aim-point selection can be performed on the basis of either engine or plume signals. In fact both, the engine and plume signals are separately recognized by the algorithm as shown in Fig. 4.

We would like to point out that the same computational scheme could be applied to data in the hyperspectral domain, i.e., one could construct covariance matrices $C_{\bar{e}}, C_{\bar{p}}, C_{\bar{s}}$, and obtain, using SVD techniques, vectors $\bar{\sigma}^{\hat{z}}(\hat{z} = \hat{e}, \hat{p}, \hat{s}, \ldots)$ upon which discrimination could be based. These possibilities have not been investigated yet. In the next section, we briefly indicate a desirable enhancement to our SVD-based scheme. Our aim is greater robustness in discrimination when processing noisy data from a low resolution (in the dynamic range sense) sensor.

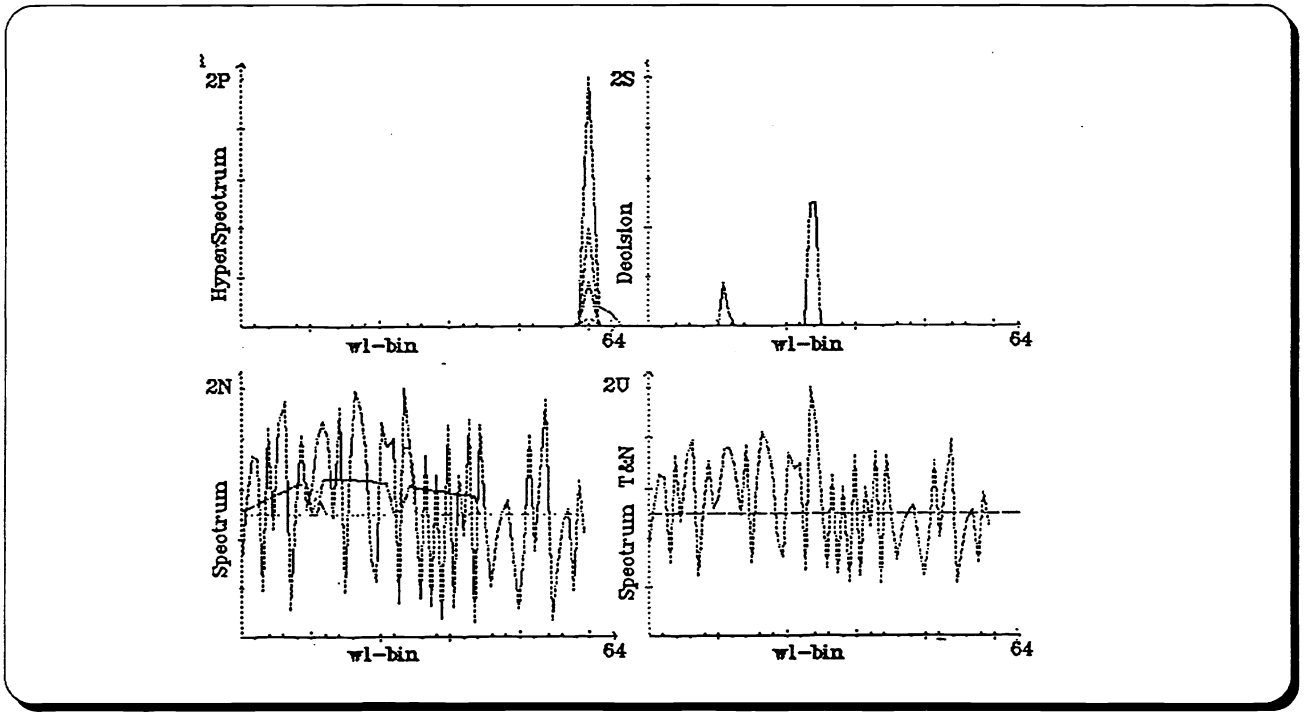

Figure 3. Engine - Plume Discrimination at S/N = -10dB (Signal Source is the Plume).

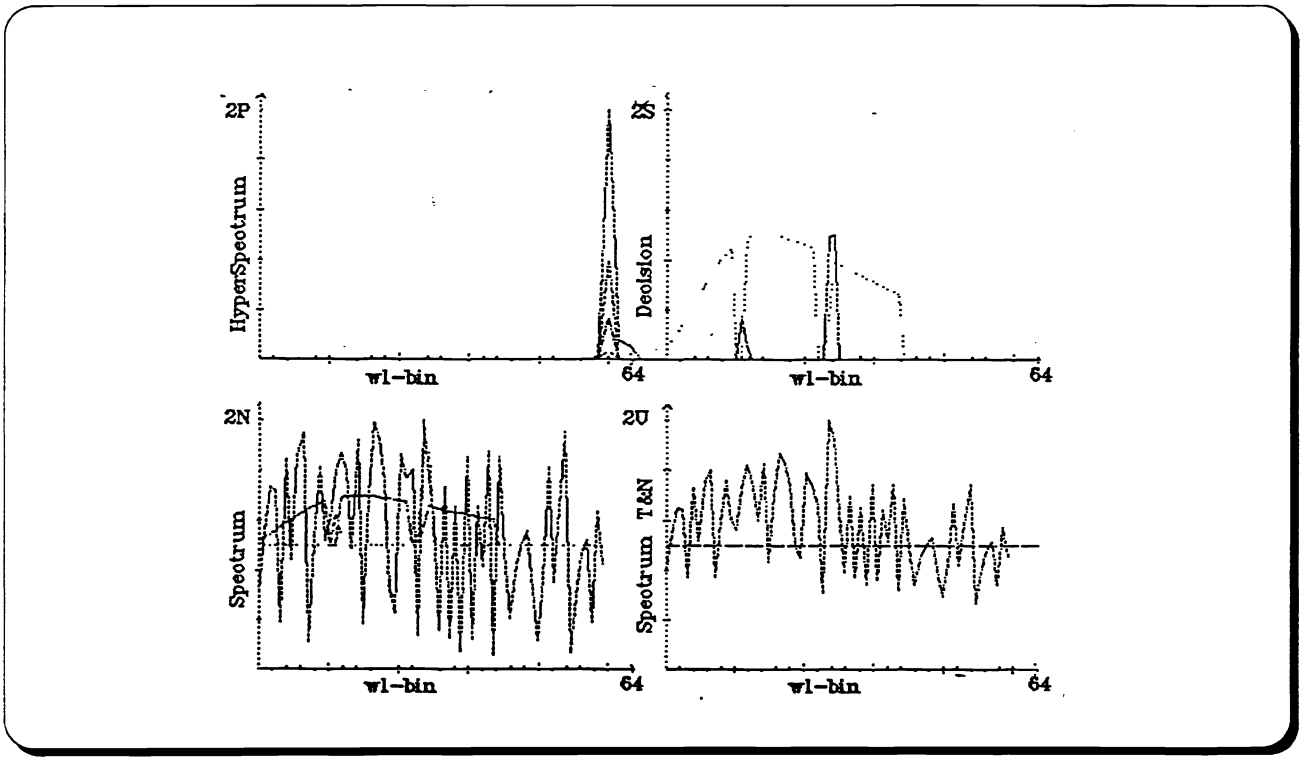

Figure 4. Engine - Plume Discrimination at S/N = -10dB (Signal Source is the Combined Plume and Engine Spectra).

2.3 Future Directions and Enhancing the Discrimination Algorithms

To proceed along the lines indicated above, we consider the following transformation:

$$q_l = \sum_{n=0}^{N-1} A_{ln} S_n^{(k)} \qquad l = 0, \ldots, L\text{-}1 \tag{16}$$

where the superscript k indexes the successive spectrometer scans, and A is a complex-valued matrix that relates information in spectral channel n to the various baseline signatures l. It is not necessary, at this stage, to specify the explicit form of the matrix elements A_{ln}. We only require A to be unitary. Let Q denote the data matrix constructed by A-filtering successive snapshots $\bar{q}^{(k)}$ of the spectrometer. Recall that $\bar{q}^H$ represents the Hermitian of $\bar{Q}$.

$$Q = \begin{Bmatrix} \bar{q}^{(1)H} \\ \cdot \\ \cdot \\ \bar{q}^{(k)H} \end{Bmatrix} \tag{17}$$

Our basic idea is to decompose Q into two orthogonal subspaces: a spectral signature subspace, and a noise subspace. Specifically, we can write

$$Q = (U_s U_\eta) \begin{pmatrix} \Sigma_s & 0 \\ 0 & \Sigma_\eta \end{pmatrix} \begin{pmatrix} V_s^H \\ V_\eta^H \end{pmatrix} \tag{18}$$

By definition of singular value decomposition we have

$$U^H U = I_u \tag{19}$$

and

$$V^H V = I_v \tag{20}$$

where I_u and I_v are identity matrices of dimensions L x L and K x K. In the absence of noise/ clutter (i.e., when $\eta = 0$), this would imply

$$A^H V_0 = 0 \tag{21}$$

When noise/clutter is present, Eq. (21) no longer holds. However, it is possible to look for the largest peaks in the inverse null spectrum

$$\frac{1}{\bar{a}^{(l)H} V_\eta V_\eta^H \bar{a}^{(l)}} \tag{22}$$

which provide the information required for the discrimination process. This approach is particularly attractive in view of the existence of analog VLSI microelectronics circuits enabling ultra-fast peak detection (i.e., "K-winners take all" neural architectures) and matrix vector multiplications (using, e.g., charge domain neural chip operating at 10^{12} ops/s/bit-of-precision), at a milliwatt power cost. The proposed approach builds upon super resolution methods developed for radar direction finding.[5]

3 SUMMARY

The concept of hyperspectral transforms domain analysis of multi- and hyperspectral signatures was introduced. Several computational schemes utilizing this concept were discussed in relation with the

discrimination problem between an airborne target and countermeasures. The algorithms have been shown to be extremely powerful, even in the presence of unusually poor signal to noise, for discrimination under a single look. Hyperspectral analyses techniques are appropriate for autonomous, intelligent, guided munitions, and may be used for subpixel targets. The same algorithms, utilizing the spectral signature of backgrounds, may be exercised to assist in the detection of targets against background and clutter.

4 REFERENCES

1. Gat, N., Barhen, J., Gulati, S., and Steiner, T.D. "The Intelligent Missile Seeker (IMS): Spectral, Spatial, and Temporal Domain-Based Target Identification and Discrimination: Part 1 -- Sensor and Discrimination Algorithms." and "Part 2 -- High Performance Intelligent Control System." Proceedings of the Third Automatic Target Recognizor System and technology Conference, Conducted at the Naval Postgraduate School, June-July, 1993. GACIAC PR-93-01, Vol. 1, Pp.117-128, and 129-139.
2. Gat, N., Barhen, J., Gulati, S., and Steiner, T.D. "Hyperspectral Imaging for Target/Decoy Discrimination: Sensor and Algorithms." Proceedings of the 1994 Meeting of the IRIS Specialty Group on Passive Sensors, March 1994, Albuquerque. Published by IRIA.
3. Barhen, J., Tomarian, N, Fijami, A., Yariv, A, and Agranot, A. "New Direction in Massively Parallel Neurocomputing in Neural Networks and Their Applications." Pp. 543-554, Proceedings of the 5th International Conference on Neural Networks and Their Applications, Nimes, France, Nov. 1992, J.C. Rault Editor, EC2 Publishers, Paris, 1992.
4. Forsythe, G.E., *et-al*, Computer Methods for Mathematical Computation, Prentice Hall, 1977.
5. Johnson, R.A., Miner, G.E., "Comparison of Superesolution Algorithms for Radio Direction Finding." IEEE Transaction AES-22, No. 4, 1986, Pp. 432-441.